Theoretical analysis on zero propellant maneuver existent conditions

Mo-Yao Yu,[1)] Ya-Zhong Luo,[1),2)] and Hai-Yang Li[2)]

College of Aerospace Science and Engineering,
National University of Defense Technology, Changsha, China

(Received Jan 10st, 2017)

Zero-Propellant Maneuver (ZPM) is an advanced concept of attitude control, which has been applied on the International Space Station. But the existence of the ZPM maneuver path has not been studied. First, dynamic models of a spacecraft using CMGs (Control Momentum Gyro, CMG) are constructed. A projection function of angular momentum is established, containing the angular momentum of spacecraft, the CMG and the gravity gradient. After that, a general energy function is deduced, which contains the kinetic energy, the gravitational potential, the centrifugal potential of spacecraft, and the energy of the gyros. Then, based on the projection function, the first ZPM existence condition is proposed by analyzing the angular momentum at initial and terminal moment of the attitude mission. Furthermore, a second condition based on the general energy function is raised, considering the threshold rotational rate of gimbal during maneuver. Effectiveness of the existence conditions is verified by path planning examples. The proposed existent conditions can provide a convenient and effective method to determine whether the ZPM path exists, which can be applied to any angle maneuver mission and can provide a significant theoretical support for zero propellant maneuver technology in the future.

Key Words: Zero-Propellant Maneuver, CMG, Existent Conditions, Energy Function

1. Introduction

Zero-propellant maneuver (ZPM) is an advanced concept of attitude control using only control moment gyroscopes (CMGs). By using CMGs, mount of propellant can be saved and gas contamination to the solar panel and other exposed device could be avoided. Moreover, it can be a backup for attitude-control thrusters. This technology will enhance orbiting lifetime of spacecraft, and improve the maneuver security and reliability effectively.

The concept of ZPM is first proposed by Bedrossian [1] at 1996. The core idea is to establish the frame of optimal control for attitude maneuver and plan maneuver path by making full use of environment torques. Then the spacecraft maneuver along the planned path using CMGs only, without any fuel consumption. On November 5. 2006, the ZPM was first demonstrated on the International Space Station (ISS). The ISS rotated 90° without consuming any propellant in 7200s. On March 3. 2007, a ZPM of 180° rotation was achieved, saving 50.76kg propellant at an estimated cost of US$1,100,000[2-3].

However, the total angular momentum that the CMGs can store is limited, and when this threshold is reached, the CMGs turn saturated. Saturation precluded CMGs from generating torques in certain direction, and may lead to the loss of attitude-control ability. Once he CMG saturate, thrusters need to work instead of CMGs. So whether the attitude maneuver mission can be achieved without CMG saturated is a judging condition for ZPM. Various approached have been explored so far to deal with the saturation problem, and most of there previous studies concentrated on the attitude stability control problems. For example, Wie used a Linear Quadratic Regulator (LQR) method to design a quadratic optimal controller for the saturation problem [4]. Vadali put forward a nonlinear controller by constructing a Lyapunov function consisting of both the attitude and momentum [5]. However, researchers seldom considered the existence of unsaturated path for a given maneuver mission. Until now, only Zhao er at gave a preliminary analysis based on the conservation of unsaturated path for a given maneuver mission. But the existence conditions proposed by Zhao can be appropriate only for attitude maneuvers between torque equilibrate attitudes, and the initial momentum of CMG is assumed to be zero, which limit the application to a great extent [6].

The existent conditions proposed in this paper can be applied to any angle maneuver mission, and there is no limitation to the initial momentum of CMGs. The main contributions of this paper are three folds: The main contributions of this paper are four folds: 1) Establish the projection function of angular momentum and the general energy function of a spacecraft with CMGs as the only actor. 2) The first ZPM existence condition is proposed by analyzing the angular momentum at initial and terminal moment. 3) The second existence condition, considering the threshold rotational rate of gimbal during maneuver is proposed. 4) The effectiveness of the existence conditions is verified by path planning examples.

2. The projection function and energy function

This investigation is focused on the spacecraft that is a finite-sized rigid body, taking a circular orbital motion. In Fig. 1, the orbital frame $Ol_1l_2l_3$ is fixed at O, the center of mass of the spacecraft. The three unit component vectors of the orbital frame are demoted as $\boldsymbol{l}_1$, $\boldsymbol{l}_2$, and $\boldsymbol{l}_3$. Vector $\boldsymbol{l}_1$ is pointing to the direction of velocity, and vector $\boldsymbol{l}_3$ points to the mass center of the Earth. The third vector $\boldsymbol{l}_2$ completes a right-handed set of orthogonal axes with $\boldsymbol{l}_1$ and $\boldsymbol{l}_3$.

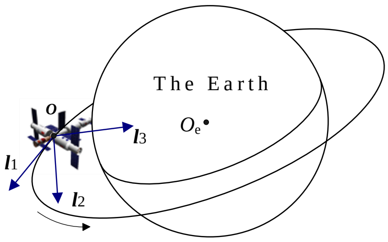

Fig. 1. The orbital frame.

The local frame $Ob_1b_2b_3$ is fixed in the rigid body, attached to O. Three unit component vectors demoted as $\boldsymbol{b}_1$, $\boldsymbol{b}_2$, and $\boldsymbol{b}_3$ are along the principal axes of inertia of the spacecraft. Principal inertias are I_1, I_2, I_3, respectively. The local frame and the orbital frame are related by yaw angle ψ, pitch angle θ and roll angle φ with a rotation sequence of 3-2-1. When the two frames are parallel, the Euler angle satisfies $\psi = \theta = \varphi = 0$. The direction cosines of axes $\boldsymbol{b}_i$ in the orbital frame $a_{ij} = \cos(l_i, \boldsymbol{b}_i)$ can be written as

$$
\begin{aligned}
&a_{11} = \cos\theta\cos\psi, a_{12} = \cos\theta\sin\psi, a_{13} = -\sin\theta \\
&a_{21} = -\cos\varphi\sin\psi + \sin\varphi\sin\theta\cos\psi \\
&a_{22} = \cos\varphi\cos\psi + \sin\varphi\sin\theta\sin\psi \\
&a_{23} = \sin\varphi\cos\theta \\
&a_{31} = \sin\varphi\sin\psi + \cos\varphi\sin\theta\cos\psi \\
&a_{32} = -\sin\varphi\cos\psi + \cos\varphi\sin\theta\sin\psi \\
&a_{33} = \cos\varphi\cos\theta
\end{aligned}
\tag{1}
$$

The elements in Eq. (1) constitute the transformation matrix $\boldsymbol{A}_{3\times3} = [a_{ij}]$ from the orbital frame to the local frame. Thus unit component vectors $\boldsymbol{l}_1$, $\boldsymbol{l}_2$, and $\boldsymbol{l}_3$ can be expressed in local frame as

$$
\begin{aligned}
\boldsymbol{l}_1 &= [a_{11}\ a_{21}\ a_{31}]^{\mathrm{T}} \\
\boldsymbol{l}_2 &= [a_{12}\ a_{22}\ a_{32}]^{\mathrm{T}} \\
\boldsymbol{l}_3 &= [a_{13}\ a_{23}\ a_{33}]^{\mathrm{T}}
\end{aligned}
\tag{2}
$$

The angular velocity of spacecraft relative to the inertial space can be divided into two parts, $\boldsymbol{\omega}_o$ and $\boldsymbol{\omega}'$, where $\boldsymbol{\omega}_o$ is the convected angular velocity, which is resulted from the orbit motion of the spacecraft, and $\boldsymbol{\omega}'$ is the spacecraft's angular velocity relative to the orbital frame. Thus, the angular velocity in local frame is

$$
\boldsymbol{\omega} = \boldsymbol{\omega}' + \boldsymbol{\omega}_o = \begin{bmatrix} \dot{\varphi} + \dot{\psi}a_{13} \\ \dot{\theta}\cos\varphi + \dot{\psi}a_{23} \\ -\dot{\theta}\sin\varphi + \dot{\psi}a_{33} \end{bmatrix} + \omega_o \boldsymbol{l}_2 \tag{3}
$$

After algebra operation, the following expressions can be get

$$
\dot{\boldsymbol{l}}_1^{\mathrm{T}} = \boldsymbol{l}_1^{\mathrm{T}}\tilde{\boldsymbol{\omega}}' = -\boldsymbol{\omega}'^{\mathrm{T}}\tilde{\boldsymbol{l}}_1 \tag{4}
$$

$$
\dot{\boldsymbol{l}}_2^{\mathrm{T}} = \boldsymbol{l}_2^{\mathrm{T}}\tilde{\boldsymbol{\omega}}' = -\boldsymbol{\omega}'^{\mathrm{T}}\tilde{\boldsymbol{l}}_2 \tag{5}
$$

$$
\dot{\boldsymbol{l}}_3^{\mathrm{T}} = \boldsymbol{l}_3^{\mathrm{T}}\tilde{\boldsymbol{\omega}}' = -\boldsymbol{\omega}'^{\mathrm{T}}\tilde{\boldsymbol{l}}_3 \tag{6}
$$

Assume that the spacecraft is influenced only by the Earth. Other environmental torques, such as aerodynamic torque, can be treated as perturbations. The attitude dynamics equation based on the theorem of moment of momentum can be expressed as

$$
\boldsymbol{I}\frac{\mathrm{d}\boldsymbol{\omega}}{\mathrm{d}t} = \boldsymbol{\tau}_{\mathrm{gyro}} + \boldsymbol{\tau}_{\mathrm{gg}} + \boldsymbol{\tau}_{\mathrm{CMG}} \tag{7}
$$

where $\boldsymbol{I}$ is the inertia matrix of the spacecraft in diagonal form. $\boldsymbol{\tau}_{\mathrm{gyro}}$, $\boldsymbol{\tau}_{\mathrm{gg}}$ and $\boldsymbol{\tau}_{\mathrm{CMG}}$ are the gyroscopic torque, the gravity gradient torque and the control torque from CMGs, respectively, taking the following forms

$$
\begin{aligned}
\boldsymbol{\tau}_{\mathrm{gyro}} &= -\tilde{\boldsymbol{\omega}}\boldsymbol{I}\boldsymbol{\omega} \\
\boldsymbol{\tau}_{\mathrm{gg}} &= 3\omega_o^2\tilde{\boldsymbol{l}}_3\boldsymbol{I}\boldsymbol{l}_3 \\
\boldsymbol{\tau}_{\mathrm{CMG}} &= -\dot{\boldsymbol{H}} - \tilde{\boldsymbol{\omega}}\boldsymbol{H}
\end{aligned}
\tag{8}
$$

where $\boldsymbol{H}$ is the angular momentum of CMGs. Thus, the Euler Equantion (7) turns to

$$
\boldsymbol{I}\frac{\mathrm{d}\boldsymbol{\omega}}{\mathrm{d}t} = -\tilde{\boldsymbol{\omega}}\boldsymbol{I}\boldsymbol{\omega} + 3\omega_o^2\tilde{\boldsymbol{l}}_3\boldsymbol{I}\boldsymbol{l}_3 - \dot{\boldsymbol{H}} - \tilde{\boldsymbol{\omega}}\boldsymbol{H} \tag{9}
$$

Euler's Eq. (9) and kinetic Eq. (3) described above together decide the attitude motion of the spacecraft using CMGs as the only actor.

1) The project function

To get the project function of angular momentum, first multiple both sides of Eq. (9) with $\boldsymbol{l}_2^{\mathrm{T}}$ in the left, then multiple Eq. (5) with $\boldsymbol{I\omega}$, $\boldsymbol{H}$ in the right, respectively. After algebra operations, the following form can be obtained

$$
\boldsymbol{l}_2^{\mathrm{T}}\boldsymbol{I}\boldsymbol{\omega} + \boldsymbol{l}_2^{\mathrm{T}}\boldsymbol{H} - 3\omega_o^2\int_{t_0}^{t_f}\boldsymbol{l}_2^{\mathrm{T}}\tilde{\boldsymbol{l}}_3\boldsymbol{I}\boldsymbol{l}_3\mathrm{d}t = \mathrm{const} \tag{10}
$$

Eq. (10) is the projection of angular momentum to the direction of $\boldsymbol{l}_2$

2) The energy function

To get the general energy function of angular momentum, first multiple both sides of Eq. (9) with $\boldsymbol{\omega}'^{\mathrm{T}}$ in the left, then multiple Eq. (5) with $\omega_o\boldsymbol{I\omega}$, $\omega_o\boldsymbol{H}$ in the right side, multiple Eq. (6) with $3\omega_o^2\boldsymbol{I}\boldsymbol{l}_3$ in the right side, respectively. Plus these equations together and after some algebra operations, the generalized integral of energy function can be obtained as

$$
\frac{1}{2}\boldsymbol{\omega}'^{\mathrm{T}}\boldsymbol{I}\boldsymbol{\omega}' - \frac{1}{2}\omega_o^2\boldsymbol{l}_2^{\mathrm{T}}\boldsymbol{I}\boldsymbol{l}_2 + \frac{3}{2}\omega_o^2\boldsymbol{l}_3^{\mathrm{T}}\boldsymbol{I}\boldsymbol{l}_3 + \omega_o^2\boldsymbol{l}_2^{\mathrm{T}}\boldsymbol{H} + \int_{t_0}^{t_f}\boldsymbol{\omega}^{\mathrm{T}}\dot{\boldsymbol{H}}\mathrm{d}t = \mathrm{const} \tag{11}
$$

Eq. (11) is actually an improved form of angular momentum of the spacecraft carrying CMGs. Terms in Eq. (11) represent the kinetic energy of spacecraft reference to the orbit, the centrifugal potential of spacecraft, the gravitational potential of spacecraft and the kinetic energy of the CMGs, respectively.

3. The boundary ZPM existent condition

3.1. Ignore environmental effect

Obviously, if ignore the effect of environment, the integral term in the project function disappears. The project function at initial and terminal moment can be denoted as

$$\begin{aligned} \boldsymbol{P}_0 &= \boldsymbol{l}_{20}^{\mathrm{T}} \boldsymbol{I} \boldsymbol{\omega}_0 + \boldsymbol{l}_{20}^{\mathrm{T}} \boldsymbol{H}_0 \\ \boldsymbol{P}_f &= \boldsymbol{l}_{2f}^{\mathrm{T}} \boldsymbol{I} \boldsymbol{\omega}_f + \boldsymbol{l}_{2f}^{\mathrm{T}} \boldsymbol{H}_f \end{aligned} \tag{12}$$

Subscript 0 and f represent initial and terminal moment, respectively. The five-pyramid SGCMG (Single Gimbal Control Momentum Gyro, SGCMG) is concerned in present research, consisting of 6 SGCMGs. The angular momentum of five-pyramid SGCMGs can be expressed as

$$\boldsymbol{H} = \left(\boldsymbol{A}\sin\boldsymbol{\delta} + \boldsymbol{B}\cos\boldsymbol{\delta}\right)\boldsymbol{E}h_0 \tag{13}$$

where h_0 is the angular momentum of a single SGCMG, $\boldsymbol{\delta}$ is diagonal matrix consist of frame angles of SGCMGs. $\boldsymbol{A}$ and $\boldsymbol{B}$ are matrixes of 3×6 dimension, decided by the install direction on the spacecraft. $\boldsymbol{E}$ is a matrix of n×1 dimension, consisted of unit values, denoted as $[1, 1 ,1, 1, 1, 1]^{\mathrm{T}}$. The derivation of angular momentum can be written as

$$\dot{\boldsymbol{H}} = \left(\boldsymbol{A}\cos\boldsymbol{\delta} - \boldsymbol{B}\sin\boldsymbol{\delta}\right)\dot{\boldsymbol{\delta}}h_0 \tag{14}$$

For a SGCMG cluster, the angular velocity of each frame is always constrained by a maximum value.

The CMGs work within its angular momentum envelope. For different configurations of SGCMG cluster, workspace can be defined together as

$$\left|\boldsymbol{H}\right| \le k_{\mathrm{CMG}} h_0 \tag{15}$$

where k_{CMG} is a coefficient decided by the configuration of SGCMG cluster. For example, the workspace for pyramid SGCMGs is $2.56 \le k_{\mathrm{CMG}} \le 3.3$, and five-pyramid SGCMGs works within $4.35 \le k_{\mathrm{CMG}} \le 4.77$. The envelope of momentum of a five-pyramid SGCMGs is almost the same as a sphere, as shown in Fig. 2.

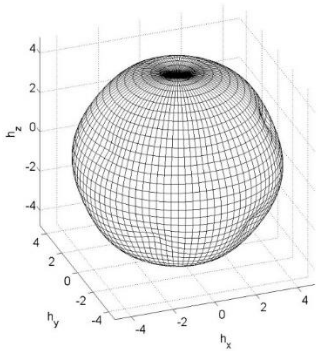

Fig. 2. The envelope of five-pyramid SGCMGs.

Once a maneuver mission is given, the initial and terminal attitude parameters are determined, including $\boldsymbol{l}_{20}^{\mathrm{T}}, \boldsymbol{l}_{2f}^{\mathrm{T}}, \boldsymbol{\omega}_0, \boldsymbol{\omega}_f$ and $\boldsymbol{H}_0$. Existence conditions can be obtained by judging whether $\boldsymbol{H}_f$ falls into the envelope in Fig. 2. When ignore the effect of environment, the initial and terminal project function equate. Thus, the following relation can be obtained

$$\boldsymbol{l}_{2f}^{\mathrm{T}} \boldsymbol{H}_f = \boldsymbol{l}_{20}^{\mathrm{T}} \boldsymbol{I} \boldsymbol{\omega}_0 + \boldsymbol{l}_{20}^{\mathrm{T}} \boldsymbol{H}_0 - \boldsymbol{l}_{2f}^{\mathrm{T}} \boldsymbol{I} \boldsymbol{\omega}_f \tag{16}$$

The right side of the Eq. (16) is a known scalar quantity. It can be known from linear algebra that when and only when vector $\boldsymbol{H}f$ is along the direction of $\boldsymbol{l}_{2f}$, the module of $\boldsymbol{H}_f$ takes a minimal value. Since $\boldsymbol{l}_{2f}$ is a unit vector, the boundary existent condition takes the following form

$$h_0 \ge \frac{\boldsymbol{l}_{20}^{\mathrm{T}} \boldsymbol{I} \boldsymbol{\omega}_0 + \boldsymbol{l}_{20}^{\mathrm{T}} \boldsymbol{H}_0 - \boldsymbol{l}_{2f}^{\mathrm{T}} \boldsymbol{I} \boldsymbol{\omega}_f}{k_{\mathrm{CMG}}} \tag{17}$$

3.2. Consider the gravity gradient torque

Environmental factors, especially gravity plays a significant role to the attitude motion of a spacecraft at low orbits. Taking the gravity gradient torque into account, the boundary project function turns to

$$\begin{aligned} \boldsymbol{P}_0 &= \boldsymbol{l}_{20}^{\mathrm{T}} \boldsymbol{I} \boldsymbol{\omega}_0 + \boldsymbol{l}_{20}^{\mathrm{T}} \boldsymbol{H}_0 \\ \boldsymbol{P}_f &= \boldsymbol{l}_{2f}^{\mathrm{T}} \boldsymbol{I} \boldsymbol{\omega}_f + \boldsymbol{l}_{2f}^{\mathrm{T}} \boldsymbol{H}_f - 3\omega_0^2 \int_{t_0}^{t_f} \boldsymbol{l}_2^{\mathrm{T}} \tilde{\boldsymbol{l}}_3 \boldsymbol{I} \boldsymbol{l}_3 \mathrm{d}t \end{aligned} \tag{18}$$

Actually, the ZPM exists most likely when the gravity gradient torque plays an assistant role to help SGCMGs absorb angular momentum of the spacecraft. In other words, the gravity gradient torque works to uninstall the SGCMGs, thus increasing the ability to exchange angular momentum with the spacecraft. This proposes the most possibility to achieve ZPM.

The concrete form of $\boldsymbol{\tau}_{\mathrm{gg}}$ in the local frame is

$$\boldsymbol{T}_g = \frac{3}{2}\omega_0^2 \begin{bmatrix} (I_3 - I_2)\sin 2\varphi \cos^2\theta \\ (I_3 - I_1)\cos\varphi \sin 2\theta \\ (I_1 - I_2)\sin 2\theta \sin\varphi \end{bmatrix} \tag{19}$$

The integral term above represents accumulative effect of energy by gravity. Put Eq. (1) into Eq. (2), the following form can be obtained

$$\boldsymbol{l}_2 = \begin{bmatrix} \cos\theta\sin\psi \\ \cos\varphi\cos\psi + \sin\varphi\sin\theta\sin\psi \\ -\sin\varphi\cos\psi + \cos\varphi\sin\theta\sin\psi \end{bmatrix}, \ \boldsymbol{l}_3 = \begin{bmatrix} -\sin\theta \\ \sin\varphi\cos\theta \\ \cos\varphi\cos\theta \end{bmatrix} \tag{20}$$

Substitute into Eq. (18), the integral term turns into

$$\begin{aligned} &3\omega_0^2 \int_{t_0}^{t_f} \boldsymbol{l}_2^{\mathrm{T}} \tilde{\boldsymbol{l}}_3 \boldsymbol{I} \boldsymbol{l}_3 \mathrm{d}t = \frac{3}{2}\omega_0^2 \int_{t_0}^{t_f} [(I_3 - I_1)\sin 2\theta\cos\psi + \\ &(I_3 - I_2)(\sin 2\varphi \sin\psi\cos\theta - \sin^2\varphi \sin 2\theta \cos\psi)]\mathrm{d}t \end{aligned} \tag{21}$$

The maximum value of is depended on the evaluation of $\boldsymbol{I}_1$, $\boldsymbol{I}_2$ and $\boldsymbol{I}_3$. Denote the maximum absolute value of $3\omega_0^2 \boldsymbol{l}_2^{\mathrm{T}} \tilde{\boldsymbol{l}}_3 \boldsymbol{I} \boldsymbol{l}_3$ as $\Delta\max$. Fig. 3 shows the change of $\Delta\max$ respect to parameters (I_3 - I_2) and ($I_3 - I_1$). From Fig. 3, it can be observed that when (I_3 - I_2) and ($I_3 - I_1$) both equals to zero, the $\Delta\max$ takes the minimum value. But when (I_3 - I_2) and ($I_3 - I_1$) takes the different sign, the value reaches its maximum.

Combining the conclusions in section 3.1, existent conditions considering gravity gradient torque can be obtained as

$$h_0 \ge \frac{\boldsymbol{l}_{20}^{\mathrm{T}} \boldsymbol{I} \boldsymbol{\omega}_0 + \boldsymbol{l}_{20}^{\mathrm{T}} \boldsymbol{H}_0 - \boldsymbol{l}_{2f}^{\mathrm{T}} \boldsymbol{I} \boldsymbol{\omega}_f - \Delta\max\left(t_f - t_0\right)}{k_{\mathrm{CMG}}} \tag{22}$$

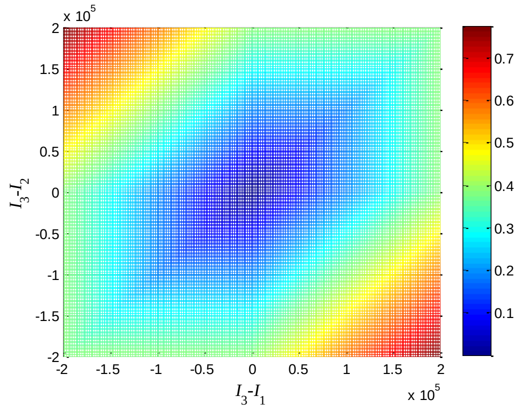

Fig. 3. The maximum value of $3\omega_0^2 \boldsymbol{l}_2^{\mathrm{T}} \tilde{\boldsymbol{l}}_3 \boldsymbol{I} \boldsymbol{l}_3$.

If the maneuver path would take the most advantages from gravity gradient torque, h_0 will take the minimum value in Eq. (22) That is to say, the gravity gradient torque will assists CMGs to complete the maneuver mission under certain case, depending on the maneuver path.

4. The process ZPM existent condition

Initial and terminal state of maneuver mission are combined to drawn the boundary conditions. Furthermore, the exchange of energy between spacecraft and CMGs during maneuver should also be taken into consideration.

In the process of maneuver, the exchange rate of energy from CMG is limited by the rotational rate of gimbal and the maximum required angular velocity of the spacecraft. Denote the threshold value of rotational rate as $\dot{\delta}_{\max}$ and the maximum required angular velocity as $\omega_{\max}$. Substitute Eq. (14) into the integral term in Eq. (11), the integral term can be written as

$$\int_{t_0}^{t_f} \boldsymbol{\omega}^{\mathrm{T}} \dot{\boldsymbol{H}} \mathrm{d}t = \int_{t_0}^{t_f} \boldsymbol{\omega}^{\mathrm{T}} \left(\boldsymbol{A} \cos \boldsymbol{\delta} - \boldsymbol{B} \sin \boldsymbol{\delta} \right) \dot{\boldsymbol{\delta}} h_0 \mathrm{d}t \tag{23}$$

As $\left(\boldsymbol{A} \cos \boldsymbol{\delta} - \boldsymbol{B} \sin \boldsymbol{\delta} \right)$ and $\left(\boldsymbol{A} \sin \boldsymbol{\delta} + \boldsymbol{B} \cos \boldsymbol{\delta} \right)$ takes the same envelope, Eq. (23) can be rearranged as

$$\int_{t_0}^{t_f} \boldsymbol{\omega}^{\mathrm{T}} \dot{\boldsymbol{H}} \mathrm{d}t \le \boldsymbol{\omega}_{\max} k_{\mathrm{CMG}} \dot{\delta}_{\max} h_0 \left(t_f - t_0 \right) \tag{24}$$

Substitute Eq. (24) into Eq. (11), the process conditions can be obtained as

$$h_0 \ge \frac{\Delta \left(\frac{1}{2} \boldsymbol{\omega}'^{\mathrm{T}} \boldsymbol{I} \boldsymbol{\omega}' - \frac{1}{2} \omega_o^2 \boldsymbol{l}_2^{\mathrm{T}} \boldsymbol{I} \boldsymbol{l}_2 + \frac{3}{2} \omega_{o3}^{2\mathrm{T}} \boldsymbol{I} \boldsymbol{I} \boldsymbol{l}_3 + \omega_o^2 \boldsymbol{l}_2^{\mathrm{T}} \boldsymbol{H} \right)_{t_0 - t_f}}{\omega_{\max} k_{\mathrm{CMG}} \dot{\delta}_{\max} \left(t_f - t_0 \right)} \tag{25}$$

To sum up in conclusion, ZPM existent conditions considering boundary and process constrains can be reorganized to the following form

$$h_0 \ge \begin{cases} \max \left\{ \dfrac{\boldsymbol{l}_{20}^{\mathrm{T}} \boldsymbol{I} \boldsymbol{\omega}_0 + \boldsymbol{l}_{20}^{\mathrm{T}} \boldsymbol{H}_0 - \boldsymbol{l}_{2f}^{\mathrm{T}} \boldsymbol{I} \boldsymbol{\omega}_f}{k_{\mathrm{CMG}}}, \dfrac{\Delta \left(\frac{1}{2} \boldsymbol{\omega}'^{\mathrm{T}} \boldsymbol{I} \boldsymbol{\omega}' - \frac{1}{2} \omega_o^2 \boldsymbol{l}_2^{\mathrm{T}} \boldsymbol{I} \boldsymbol{l}_2 + \frac{3}{2} \omega_{o3}^{2\mathrm{T}} \boldsymbol{I} \boldsymbol{I} \boldsymbol{l}_3 + \omega_o^2 \boldsymbol{l}_2^{\mathrm{T}} \boldsymbol{H} \right)_{t_0 - t_f}}{\omega_{\max} k_{\mathrm{CMG}} \dot{\delta}_{\max} \left(t_f - t_0 \right)} \right\}, & \text{Ignore gravity} \\ \max \left\{ \dfrac{\boldsymbol{l}_{20}^{\mathrm{T}} \boldsymbol{I} \boldsymbol{\omega}_0 + \boldsymbol{l}_{20}^{\mathrm{T}} \boldsymbol{H}_0 - \boldsymbol{l}_{2f}^{\mathrm{T}} \boldsymbol{I} \boldsymbol{\omega}_f - \Delta \max \left(t_f - t_0 \right)}{k_{\mathrm{CMG}}}, \dfrac{\Delta \left(\frac{1}{2} \boldsymbol{\omega}'^{\mathrm{T}} \boldsymbol{I} \boldsymbol{\omega}' - \frac{1}{2} \omega_o^2 \boldsymbol{l}_2^{\mathrm{T}} \boldsymbol{I} \boldsymbol{l}_2 + \frac{3}{2} \omega_{o3}^{2\mathrm{T}} \boldsymbol{I} \boldsymbol{I} \boldsymbol{l}_3 + \omega_o^2 \boldsymbol{l}_2^{\mathrm{T}} \boldsymbol{H} \right)_{t_0 - t_f}}{\omega_{\max} k_{\mathrm{CMG}} \dot{\delta}_{\max} \left(t_f - t_0 \right)} \right\}, & \text{Consider gravity} \end{cases} \tag{26}$$

5. Simulations

To verify the correctness of the proposed existent conditions, a large amount of simulations have been carried out for both situations that ignoring and considering the environmental effects.

5.1. Situation 1: Small-angle maneuver missions

Assume that the spacecraft flies in a circular orbit with an altitude of about 380 km, and the primary inertia of the spacecraft is diag[3 5 8]×10^6 kg.m^2. According to the deduced existent conditions, the minimum value of h_0 in different small-angle maneuver missions are listed in Tab. 1.

To insure the proper operation of SGCMGs, the forecast of saturation is usually necessary. The most commonly used indicator to measure the degree of saturation is the saturation-value, denoted as

$$d = \det(QQ^{\mathrm{T}}) \tag{27}$$

where $\boldsymbol{Q} = \boldsymbol{A} \cos \boldsymbol{\delta} - \boldsymbol{B} \sin \boldsymbol{\delta}$. When the SGCMGs turn or approach saturation, the value of d will be 0 or extremely approach 0. Under this situation, the SGCMGs can't work normally. Choose angular momentum h_0 of a single SGCMG as variety and change the value of h_0 in the neighborhood of the marginal value. Figure 4 shows the minimum value of d during the 4 attitude missions, where the maneuver path is planned by pseudo-spectral method [7-9].

Table 1. Parameters of small-angle maneuver missions.

	$[\psi_s,\theta_s,\varphi_s]$ (°)	$[\psi_f,\theta_f,\varphi_f]$ (°)	Δt (s)	h_0 (N.m.s) (ignore)	h_0 (N.m.s) (consider)
1	[0 0 0]°	[0 0 5]°	200	251.4	223.3
2	[0 0 0]°	[0 10 0]°	200	289.9	267.1
3	[0 -5 0]°	[5 0 0]°	200	278.4	256.3
4	[5 0 0]°	[0 0 -5]°	200	264.9	289.1

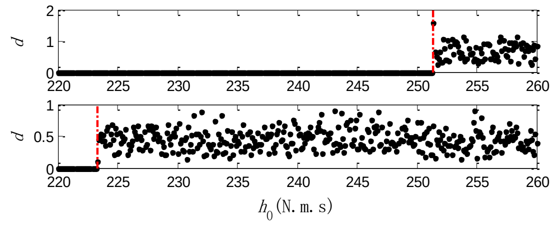

(a) The No. 1 maneuver mission.

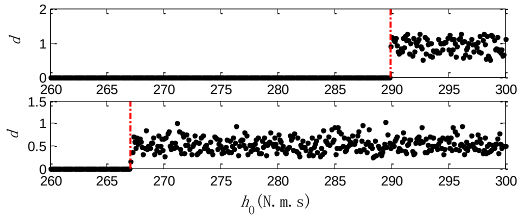

(b) The No. 2 maneuver mission.

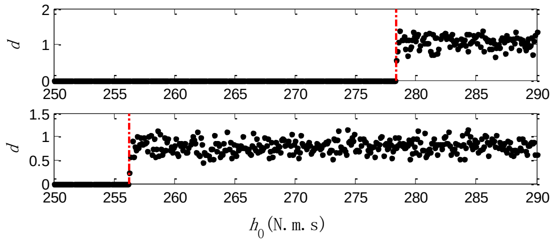

(c) The No. 3 maneuver mission

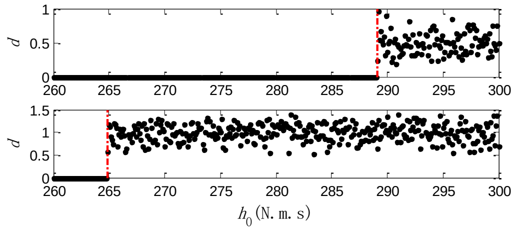

(d) The No. 4 maneuver mission

Fig. 4 The change of saturation-value for the 4 maneuver missions.

Fig. 4 shows the changing of singular-values during the maneuver missions. It can be discovered that no matter ignore or consider the effect of gravity, when h_0 is smaller than the marginal value, the minimum value of d is always zero, which means that saturation occurs during the maneuver. Along with the grow of h_0, the minimum value of d changes larger, keeping away from zero. It shows that no saturation seems to happen as h_0 grows larger than the marginal value. The simulation results verified the proposed existence conditions well. Compared with the two situations in each attitude mission, it can be discovered that the marginal momentum of a single SGCMG is always smaller when considering gravity gradient torque due to its assistant effect during maneuver.

5.2. Situation 2: Large-angle maneuver missions

Suppose the orbital and inertia parameters are the same with **Situation 1**. Different from **Situation 1**, some large-angle maneuver missions are listed in Tab. 2. This maneuver missions contains typical yaw, roll, pitch maneuver and some other random missions. According to the deduced existent conditions, the minimum value of h_0 in different maneuver missions are also listed.

Table 2. Parameters of large-angle maneuver missions.

	$[\psi_s, \theta_s, \varphi_s]$ (°)	$[\psi_f, \theta_f, \varphi_f]$ (°)	Δt (s)	h_0 (N.m.s) (ignore)	h_0 (N.m.s) (consider)
1	[0 0 0]°	[0 0 90]°	1000	560.4	543.3
2	[0 0 0]°	[0 180 0]°	1000	478.3	437.1
3	[-45 0 0]°	[0 0 130]°	1000	789.4	656.4
4	[5 120 0]°	[-6 0 30]°	1000	810.3	745.1

Fig. 5 shows the minimum value of d during the 4 attitude missions. The variation trend of the curves is similar with that in Fig. 4. It can be discovered that the saturation indicator d goes away from zero slower than the curves in Fig. 4. That's because during the large-angle mission, the exchanged angular momentum may run into some peak value that can't reflected in the boundary conditions. Thus, for large-angle maneuver missions, some spare momentum should be left to ensure the achievement of large-angle maneuver mission.

6. Conclusion

In this study, existence conditions for zero-propellant maneuver are proposed according to the deduced project function and energy function. First, dynamic models of spacecraft using control momentum gyros are constructed, based on which the project function and general energy function is established. Then the first ZPM existence condition is proposed by analyzing the projection of angular momentum at the initial and terminal moment. Furthermore, a second condition is raised, considering angular velocity and the threshold rotational rate of gimbal during maneuver. Effectiveness of the existence conditions is verified by path planning examples. The proposed existence conditions can provide a convenient and effective method to determine whether the ZPM path exists, which can be applied to any angle maneuver assignment and can provide significant theoretical support for zero propellant maneuver technology in the future..

Acknowledgments

The authors acknowledge financial support from the National Natural Science Foundation of China (No. 11572345, 11222215)

References

1) Bedrossian, N., Metzinger, R., Adams, N.: Centralized Momentum Management, Draper Lab Presentation, 1996.
2) Bedrossian, N., Bhatt, S., Lammers, M. and Nguyen, L.: Zero-Propellant Maneuver TM Flight Results for 180 deg ISS Rotation, *Proceedings of the 20th International Symposium on Space Flight Dynamics*, 2008.
3) Kang, W., Bedrossian, N.: Pseudospectral Optimal Control Theory Makes Debut Flight, Saves NASA $1 M in Under Three Hours. *SIAM News*, 2007, 40(7)
4) Wie, B., Byun, K. W., Warren, W., Geller D., et al. A New Momentum Management Controller for the Space Station, *Journal of Guidance, Control, and Dynamics*, 1989, 12(5): pp. 714-722.

5) Vadali, S. R., Oh, H.S.: Space station attitude control and momentum management: a nonlinear look, AIAA-90-3353, 1992.
6) Zhao Qian, Huang Haibing and Li yi.: Zero propellant maneuver path existence analysis for space station, *Journal of national university of defense technology*, 2015, 37(1): pp. 59-64.(In Chinese).
7) Elnagar, G., Kazemi, M. A. and Razzaghi, M.: The pseudospectral legendre method for discretizting optimal control problems, IEEE Transaction on Automatic Control, 1995, 40(10): pp. 793-1796.
8) Gong, Q., Ross, I. M. and Fahroo, F.: Spectral algorithm for pseudospectral methods in optimal control, *Journal of Guidance Control and Dynamics*, 2008, 31(3): pp. 460-471.
9) Rao, A. V.: A Survey of Numerical Methods for Optimal Control, AAS/AIAA Astrodynamics Specialist Conference, Pittsburgh, PA, 2009, AAS Paper 09-334.